Atmospheric Environment 124 (2016) 55–63

Contents lists available at ScienceDirect

Atmospheric Environment

journal homepage: www.elsevier.com/locate/atmosenv

Potential application of VIIRS Day/Night Band for monitoring nighttime surface $PM_{2.5}$ air quality from space

Jun Wang [a, *], Clint Aegerter [a], Xiaoguang Xu [a], James J. Szykman [b]

[a] Department of Earth and Atmospheric Sciences, University of Nebraska, Lincoln, NE, USA
[b] National Exposure Research Laboratory, U.S. Environmental Protection Agency, RTP, NC, USA

HIGHLIGHTS

- VIIRS Day/Night Band (DNB) is much more sensitive to aerosols than to water vapor
- Modeling of outdoor light transfer in nighttime atmosphere for VIIRS DNB
- DNB potential for estimating surface $PM_{2.5}$ is shown qualitatively and quantitatively
- $PM_{2.5}$ at VIIRS night overpass time is much closer to daily-mean $PM_{2.5}$ than at daytime
- Strategies for future DNB remote sensing of aerosols are elaborated

ARTICLE INFO

Article history:
Received 7 April 2015
Received in revised form
4 November 2015
Accepted 5 November 2015
Available online 10 November 2015

Keywords:
Nighttime
PM2.5
VIIRS
Day/Night Band

ABSTRACT

A pilot study is conducted to illustrate the potential of using radiance data collected by the Day/Night Band (DNB) of the Visible Infrared Imaging Radiometer Suite (VIIRS) aboard the Suomi National Polar-orbiting Partnership (S-NPP) satellite for particulate matter (PM) air quality monitoring at night. The study focuses on the moonless and cloudless nights in Atlanta, Georgia during August–October 2012. We show with radiative transfer calculations that DNB at night is sensitive to the change of aerosols and much less sensitive to the change of water vapor in the atmosphere illuminated by common outdoor light bulbs at the surface. We further show both qualitatively that the contrast of DNB images can indicate the change of air quality at the urban scale, and quantitatively that change of light intensity during the night (as characterized by VIIRS DNB) reflects the change of surface $PM_{2.5}$. Compared to four meteorological variables (u and v components of surface wind speed, surface pressure, and columnar water vapor amount) that can be obtained from surface measurements, the DNB light intensity is the only variable that shows either the largest or second largest correlation with surface $PM_{2.5}$ measured at 5 different sites. A simple multivariate regression model with consideration of the change of DNB light intensity can yield improved estimate of surface $PM_{2.5}$ as compared to the model with consideration of meteorological variables only. Cross validation of this DNB-based regression model shows that the estimated surface $PM_{2.5}$ concentration has nearly no bias and a linear correlation coefficient (R) of 0.67 with respect to the corresponding hourly observed surface $PM_{2.5}$ concentration. Furthermore, ground-based observations support that surface $PM_{2.5}$ concentration at the VIIRS night overpass (~1:00 am local) time is representative of daily-mean $PM_{2.5}$ air quality ($R = 0.82$ and mean bias of -0.1 μg m^{-3}). While the potential appears promising, mapping surface $PM_{2.5}$ from space with visible light at night still face various challenges and the strategies to address some of these challenges are elaborated for future studies.

1. Introduction

The last decade has seen a growing interest of applying satellite remote sensing data to derive mass concentration of aerosol or particulate matter at the surface (Wang and Christopher, 2003; Liu

* Corresponding author. 303 Bessey Hall, Lincoln, NE, 68588, USA.
E-mail address: jwang7@unl.edu (J. Wang).

http://dx.doi.org/10.1016/j.atmosenv.2015.11.013
1352-2310/

et al., 2004; Hoff and Christopher, 2009; van Donkelaar et al., 2013). Surface Particulate Matter (PM) concentration is a primary standard for evaluating air quality, and improved estimates of the spatial distribution from satellite data, if accurate, can enhance the ground-based aerosol observation network and provide an improved understanding of spatial gradients of PM for air quality assessment at the regional to continental scale. Indeed, operational monitoring of particulate matter (PM) with aerodynamic diameters less than 2.5 μm ($PM_{2.5}$) does not exist in many developing countries such as China and India (Hoff and Christopher, 2009), even though it has been known for decades that increased exposure to $PM_{2.5}$ can induce respiratory diseases and premature death (Wilson and Spengler, 1996).

While the air quality standards for PM vary in different countries, the standards are often expressed in terms of surface dry PM mass concentration at 24-h or annual averages, which contrasts with an instantaneous aerosol optical measurement derived from radiances at the satellite overpass time. For example, the most recent primary National Ambient Air Quality Standards (NAAQS) for $PM_{2.5}$ promulgated by U.S. EPA set the daily standard at 35 μgm^{-3} (24-hr average) and the annual standard at 12 μgm^{-3}. At the vast majority of surface $PM_{2.5}$ monitors used to determine compliance with these standards, the method is based on an integrated (24-h) filter-based measurement operated every 3rd day. There are also continuous $PM_{2.5}$ monitoring methods which provide hourly $PM_{2.5}$ measurements, with the vast majority being used to supply data to support development of air quality models and forecasts, including the Air Quality Index (AQI). Regardless of the type monitor or use of data, additional information on both the temporal and spatial distribution of $PM_{2.5}$ can fill gaps in the assessment of air quality conditions.

This study introduces the first attempt to derive the near-surface $PM_{2.5}$ at night from the visible lights measured by the Day/Night Band (DNB) on the VIIRS sensor aboard the NPP satellite launched in October 2011. VIIRS views the Earth at 22 channels, including 9 bands (in addition to DNB) in the visible to near infrared (IR) spectrum, 8 bands in middle IR and 4 bands in thermal IR (Lee and Miller, 2006). With its swath of ~3000 km at the equator, VIIRS provides global coverage twice within 24 h. Similar to its predecessor, the Operational Linescan System (OLS) that has been aboard the DMSP for detecting clouds and city lights during night (Elvidge et al., 1999), the VIIRS DNB has a spectral width covering 0.4–0.9 μm. Different from OLS, which has only 6-bit quantization, a nominal footprint of 2 km at nadir, and no onboard calibration, VIIRS DNB has 3-level of gains (for low, medium, and high intensity light) respectively digitized with 13, 13, and 14-bits, onboard calibration, and a nearly constant resolution of ~750 m across the scan swath (Lee and Miller, 2006). Such advanced capability in DNB provides an unprecedented opportunity to monitor visible light during night from space. While past case studies have used artificial light from OLS and DNB to derive aerosol optical depth at night (Zhang et al., 2008; Johnson et al., 2013), the application of the VIIRS DNB for nighttime PM air quality applications is still unexplored because the operational retrieval of AOD from VIIRS is only conducted during daytime by using radiance data at shortwave spectrum (Jackson et al., 2013).

Estimates of surface $PM_{2.5}$ at night from space are important for various reasons. First, surface $PM_{2.5}$ often has a distinct diurnal cycle, and hence satellite-based estimate of surface $PM_{2.5}$ at night can be used together with other remote sensing techniques that rely on sunlight to estimate daily-averaged PM (Wang and Christopher, 2003; Liu et al., 2004; Al-Saadi et al., 2005; Gupta et al., 2006; P. Gupta et al., 2006; Engel-Cox et al., 2013; van Donkelaar et al., 2013). Second, factors that regulate the surface PM at night often highly contrast with their counterparts during daytime; these factors include a shallow nocturnal boundary layer, low efficiency in oxidation and gas-to-particle conversion, weak turbulent mixing (sometimes further suppressed by temperature inversion), and largely reduced emissions from human activity such as transportation, cooking, construction, etc. (Seinfeld and Pandis, 2006). Observation-constrained assessments of the relative importance of these factors are highly needed for a better understanding of the change of surface daily $PM_{2.5}$ mass, but currently are hindered by the fact that operational retrievals of aerosols from space are made most often during daytime (with an exception of using lidar such as CALIOP that often has limited spatial coverage, Winker et al. (2002)).

At night, artificial lights and moonlight are two major sources for the visible lights. While the spatiotemporal distribution of incoming moonlight at the top of atmosphere can be much better quantified than artificial lights (Miller and Turner, 2009), the intensity of artificial lights, especially in an urban environment, is generally more stable and a factor of 10 higher than moonlight (Miller and Turner, 2009). Hence, in this study, we will explore the potential of using city lights in a large urban center (Atlanta) to derive the surface $PM_{2.5}$ at night. In addition, the intensity of city lights is also shown to be a good indicator of city population and energy consumption (Elvidge et al., 1999), and hence, the process of using city lights to derive surface $PM_{2.5}$ can fit the emergent needs for operational air monitoring in urban regions where the NAAQS are often not in compliance (such as the Atlanta Metropolitan Statistical Area or MSA). Through a case study, this paper is aimed to introduce the potential of VIIRS DNB for nighttime PM estimate to the air quality community, and to elaborate on the challenges of the next steps. We present data and our approach in Section 2, analysis in Section 3, and conclude our paper in Section 4.

2. Data and approach

2.1. Data and DNB sensitivity to aerosol and water vapor

Located aboard S-NPP, the VIIRS is a 22-band scanning radiometer with a nominal spatial resolution of 375 m in the five imagery bands (I-bands) and 750 m in both the 16 moderate-resolution bands (M-bands) and the day–night band (DNB) (Polivka et al., 2015). Over a single orbit, the intensity of visible light that VIIRS encounters can range seven orders of magnitude (from daytime cloud reflection of solar radiation to nighttime illumination by airglow, starlight, and zodiacal light in clear sky conditions) (Lee and Miller, 2006). To achieve high radiometric resolution across such a large dynamical range of visible light, DNB is deigned to: (a) have a broad spectral coverage (of 0.4–0.9 μm and half width and half maxima of the spectral response function at 0.7 μm, Fig. 1), and (b) select its amplification gain dynamically from three simultaneously collecting stages (groups of detectors) (Lee et al., 2006). Each of three stages (corresponding to high, medium, and low gains, respectively) covers a radiance range of more than 500:1 and has generous overlap with its adjacent stage(s) to ensure a good single-to-noise ratio (Lee et al., 2006). In average, DNB's *radiometric* uncertainties are estimated as 3.5%, 7.8%, and 11.0% during daytime, twilight, and nighttime conditions, respectively (Miller et al., 2012). With such accuracy, DNB data is shown to be valuable for studying meteorological and surface features illuminated by moonlight as well as for detecting airglow structures in the mesosphere at night (Miller et al., 2012).

The VIIRS sensor data records (SDRs) of calibrated radiances and brightness temperatures cover a spectral range from 0.411 to 11.87 μm and are used in a wide range of Earth observation applications, including fire detection and characterization, retrieval of cloud and aerosol properties, and land and sea surface

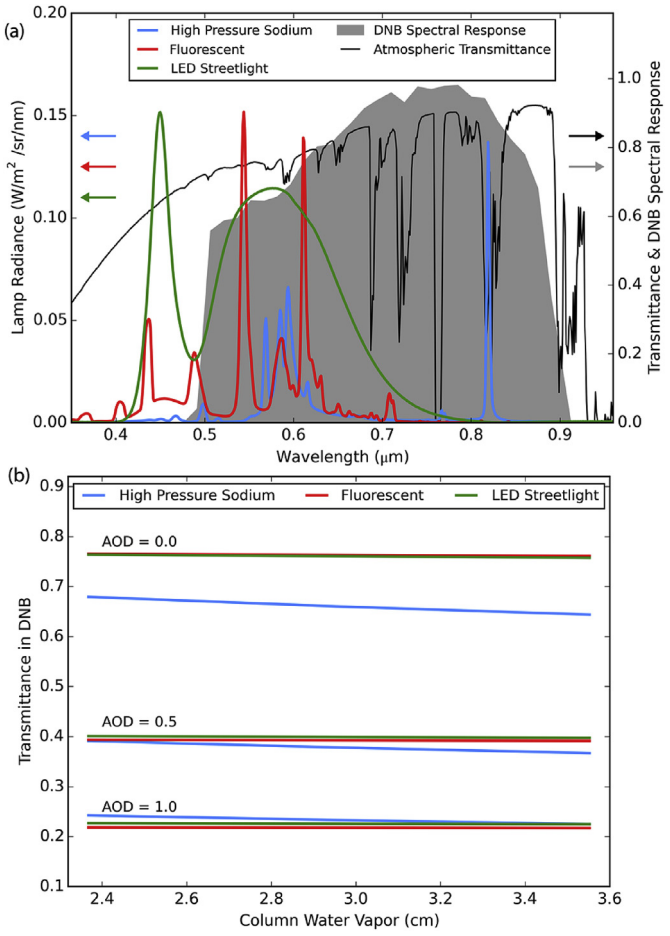

Fig. 1. (a) DNB spectral response function (shaded grey area) and atmospheric transmittances (black line for AOD = 0) overlaid with the emission spectra of commonly used city lamps: (70-Watt) high pressure sodium lamp (HPS, blue line), standard (32-Watt) fluorescent tube (red line), and 100-Watt natural-white LED streetlight lamp (green line). (b) atmospheric transmittance integrated over DNB as a function of columan water vapor amount (e.g., precipitable water) for three different surface conditions (illuminated by HPS, fluorescent, and LED lampls, respectivley) and three aerosol conditions (with AOD of 0, 0.5, and 1 at 0.55 μm). The simulation is conducted with UNified and Linearized Vector Radiative Transfer Model (UNL-VRTM, Wang et al., (2014)) for the standard mid-latitude summer atmospehric profile. Aerosol properties are based on Dubovik et al., (2002) for urban aerosols. The database of spectral intensity emitted from HPS, fluorescent, and LED bulbs are from Elvidge et al., (2010).

temperature estimation (Cao et al., 2013). For this study, three VIIRS datasets are used: (a) VIIRS DNB scientific data record (SDR) that includes DNB radiances (Cao et al., 2013); (b) VIIRS DNB geolocation SDR that includes the latitude, longitude, moonphase angle, and Moon-Sun-Earth-Satellite geometries (Cao et al., 2013); (c) VIIRS cloud mask intermediate product (CVM) (Kopp et al., 2014). In addition, VIIRS night imagery is also used to filter out the days that have clouds.

In total, 15 moonless and cloudless nights of data are found from 1 August 2012 to 30 October 2012. Hourly $PM_{2.5}$ data were extracted from the Environmental Protection Agency (EPA) Air Quality System (AQS) Data Mart for 5 Georgia Department of Natural Resources (GADNR) continuous $PM_{2.5}$ monitoring stations within Atlanta, Georgia. 3 sites (denoted as A, B, and C in Fig. 2) are in the Atlanta suburb region and 2 sites (D and E) are in the Atlanta urban center. Table 1 lists each site (A-E) AQS site ID, location, county and monitor type. Furthermore, the $PM_{2.5}$ mass averaged over these 5 sites is used to represent the mean state of the PM air quality in Atlanta, and it is compared to the light intensity averaged over the core of the urban center (i.e., CTR site denoted as F in Table 1 and Fig. 2).

In the moonless mid-night (the VIIRS overpass time), the outdoor lights are the dominate source for the broadband radiance measured by DNB, although airglow and star lights can also been seen in the DNB image (Miller and Turner, 2009). However, the spectra of outdoor lights can highly vary, depending on the color temperature of (and in many cases gases inside) the light bulb, as well as the bulb variety (Elvidge et al., 2010). In the U.S., high-pressure sodium lamps (HPS) are the most common type of light source used for outdoor applications (Rea et al., 2009), while fluorescent and light-emitting diode (LED) lamps are also often used. By comparing the spectral radiances emitted from these three types of lamps (the color lines of Fig. 1a) with the spectral transmittance of cloud-free and aerosol-free mid-latitude summer atmosphere (the grey line in Fig. 1a) in the DNB spectrum, we find that the radiances from outdoor lamps are primarily in the visible spectrum less than 0.65 μm, and hence, their transfer within the atmosphere are not affected by the major gas absorption lines (such as 0.69 μm of O_2 B, 0.76 μm of O_2 A, 0.72 μm and 0.82 μm of water vapor). We note that HPS lamp does have an emission peak coincident at 0.82 μm of water vapor absorption, but both the width of this peak emission and the water vapor line are very narrow (<3 nm) with respect to the broad spectrum of DNB.

Overall, our calculation (after integrating the spectral transmittance, lamp spectral intensity, and DNB response function) reveals that the change of water vapor has negligible effect on the DNB transmittance in the atmosphere (or the atmospheric radiative transfer that affects DNB signal). Regardless of aerosol loading, variation of preciptitable water by 40% results in a maximum change of DNB transmittance by ~1% when the light source is from HPS (Fig. 1b). In contrast, a change of AOD from 0.0 to 0.5 and 1.0 at 0.55 μm can lead to the change of DNB transmittance by ~30% and ~28%, respectively (Fig. 1b). Interestingly, Fig. 1b also shows that as AOD increases (from 0 to 1), the DNB transmittance decrease is smaller for HPS spectra (blue line) than for LED or fluorescent spectra (e.g., red or green line). This smaller decrease is due to the enhanced multiple scattering of aerosols (associated with the increase of AOD) that is larger and thus renders more decrease of transmittance in shorter wavelengths (<0.7 μm) where the radiances emitted from LED and fluorescent bulbs are mostly concentrated. Hence, the relative contribution of emission at wavelengths larger than 0.7 μm (such as in the case of HPS) is becoming larger as AOD increases, which explains why in Fig. 1b, for AOD = 0 blue line is below, and for AOD = 1 blue line is above the red and green lines.

2.2. Assumptions and regression approach

While our analysis in Fig. 1 suggests that the DNB is sensitive to the change of atmospheric aerosols (and is much less sensitive to the change of water vapor), accurate modeling of the light transfer in the night can be further complicated by the surface conditions, especially how the light from lampas interacts with surfaces and buildings. Here, as the exploratory first step, we make the same assumption as Zhang et al. (2008) that the upward visible radiation from the surface layer (including surface canopy, buildings, streets, etc.) is Lambertian and has a constant intensity of I_0 for a given location during our 3-month study period. In this assumption, the surface canopy and buildings are considered as one surface layer, and I_0 is the intensity of light at the top of surface layer entering into the atmosphere. Hence, I_0 is not exactly equal to the intensity of light at the ground and is a result of multiple scattering and reflection of lights between air and buildings within the surface layer. I_0 is expected to be strongest in places with intense lights at

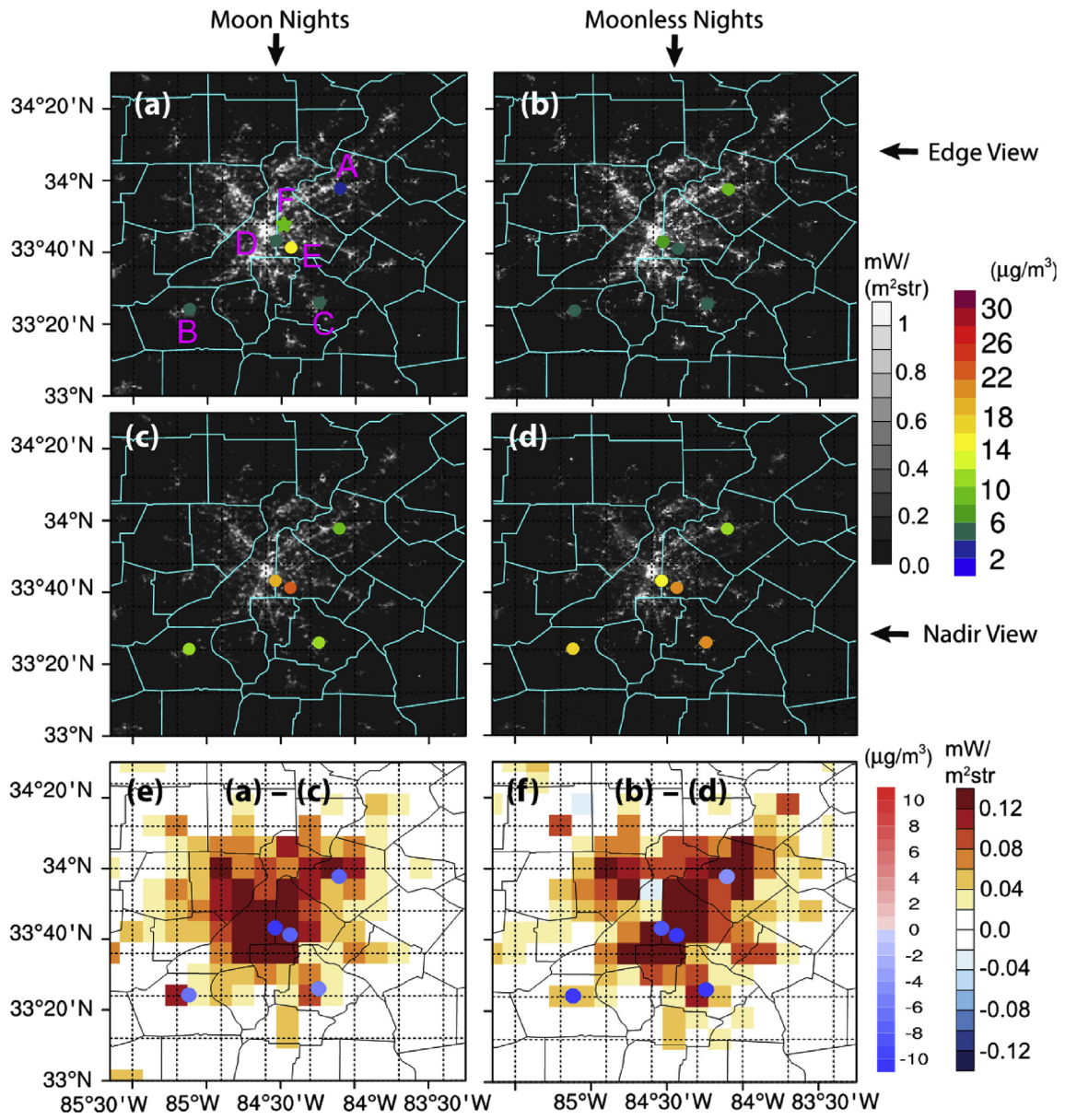

Fig. 2. (a)–(d): images of VIIRS DNB radiances for Atlanta city on 24 Sep., 15 Sep., 25 Oct., and 17 Aug. 2012 respectively; solid circles denote the location of 5 EPA $PM_{2.5}$ monitoring sites color coded with the measured $PM_{2.5}$ mass concentration during the satellite overpass time. For (a), the satellite viewing zenith angle θ and the moonphase angle η are 46.90°, and 59.36°, respectively; the set of these angle values for (b), (c), and (d) are (50.60°, 152.04°), (9.55°, 52.22°), and (1.45°, and 173.36°) respectively. (e): the difference between (a) and (c). (f): same as (e) but for (b) and (d). Note the data are gridded into 0.03° resolution in (e) and (f).

the ground (such as city centers) and weaker in suburb areas. However, at a specific location, we can reasonably assume that surface features (such as layout of buildings and location of lights) don't change within 3 months in a particular year; consequently, in the following analysis, I_0 is treated as a constant for each location within VIIRS pixel, but is allowed vary spatially.

Table 1
Summary information of the 5 Georgia DNR continuous $PM_{2.5}$ sites.

Site	AQS site ID	County	Longitude	Latitude	$PM_{2.5}$ Monitor type[a]
A	131350002	Gwinnett	−84.069	33.961	R&P TEOM Series 1400
B	130770002	Coweta	−84.746	33.404	R&P TEOM Series 1400
C	131510002	Henry	−84.161	33.433	R&P TEOM Series 1400
D	131210055	Fulton	−84.357	33.720	R&P TEOM Series 1400
E	130890002	DeKalb	−84.290	33.688	MetOne BAM-1020
F(CTR)[b]	N/A[b]	N/A[b]	−84.39	33.75	N/A[b]

[a] A measurement intercomparison between BAM (β-ray Attenuation Monitor) and TEOM (Tapered Element Oscillating Microbalance) monitors conducted by Schwab et al., 2006 revealed high correlation of 0.96 and low standard errors of 0.02 and 0.33 associated with slope (~1.02) and intercept (~1.72), respectively (Schwab et al., 2006).
[b] Site F is the center of study area, and its $PM_{2.5}$ concentration is computed by averaging the hourly $PM_{2.5}$ mass concentration measured at the sites A-E. See text for details.

By neglecting multiple scattering (the same strategy as Zhang et al. (2008)), the radiance I that DNB measures for an atmospheric optical depth τ at viewing angle with its cosine value of μ is:

$$I = I_0 e^{-\tau/\mu} \quad (1)$$

We further assume that the profile of aerosol extinction coefficient follows a well-defined structure in the nocturnal boundary layer, so that the optical depth (or total extinction) can be related to the surface extinction coefficient by an effective height H (Wang and Christopher, 2003):

$$\tau_{aer} = PM_{2.5} f(rh) Q_{mext} H \quad (2)$$

where Q_{mext} is the mass extinction efficiency at dry conditions, and $f(rh)$ is the correction factor for relative humidity impact on aerosol size and refractive index, and hence aerosol extinction efficiency, due to particle hygroscopic growth (Wang and Martin, 2007). As in Kessner et al. (2013), H is mathematically defined as the integral of the shape of aerosol extinction profile in an atmospheric column. By combining equations (1) and (2), we obtain:

$$\frac{PM_{2.5} f(rh) Q_{mext} H}{\mu} + \tau_{Ray} + \tau_{gas} = ln(I_0) - ln(I) \quad (3)$$

To the first order, the Rayleigh scattering optical depth τ_{Ray} is linearly proportional to the surface pressure (P_s by a factor of b_p), while the optical depth due to gas absorption τ_{gas} is linearly proportional to the precipitable water vapor amount (W) by a factor of b_w (Liou, 2002). Hence, equation (3) can be re-written as:

$$\frac{PM_{2.5} f(rh) Q_{mext} H}{\mu} = ln(I_0) - ln(I) - b_w \times W - b_p \times P_s \quad (4)$$

where subscripts w and p denotes water vapor and pressure, respectively.

We apply equation (4) over the 5 ground-based GADNR sites and the CTR site to evaluate practical robustness of equation (4). At each of these sites, we obtain the surface pressure data from weather stations in Atlanta, column water vapor amount from MODIS observations (King et al., 2003), $PM_{2.5}$ mass from ground-based observations, μ and I from DNB data. However, $f(rh)$, Q_{mext}, and H are not directly measured, and hence, have to be either directly assumed or determined from atmospheric chemistry transport models. We model $f(rh)$ based upon the parameterization used by Interagency Monitoring of Protected Visual Environments (IMPROVE) for the fall season in this region (Malm et al., 1994), noting that ammonium sulfate dominates the particle compsition in this region. Q_{mext} and H depend respectively on aerosol composition and boundary layer height (or turbulent mixing) and thus vary with time. However, we found that using Q_{mext}, RH, and H from a chemistry transport model (such as WRF-Chem) did not improve the results that we obtained in the regression analysis (Section 3) assuming that the product of Q_{mext} and H are constant and using the hourly RH data reported by National Weather Service in Atlanta. Since the accurate values of Q_{mext} and H are not available from *in situ* measurements, we treat the Q_{mext} and H as constants in our following analysis, with an acknowledgment that such simple treatment should be improved once we have more *in situ* data about these parameters. Consequently, equation (4) becomes

$$\frac{PM_{2.5} f(rh)}{\mu} = a_0 - a_I ln(I) - a_r \times W - a_p \times P_s \quad (5)$$

where a_0, a_I, a_r, and a_p are linear coefficients, and vary with space and time

While equation (5) establishes the link between surface $PM_{2.5}$ and the intensity of light measured by the DNB, $PM_{2.5}$ concentration at night over a particular location is traditionally modeled without use of any DNB data, and its day-to-day change can be affected by meteorological factors such as wind speed and wind direction. Hence, after deriving $PM_{2.5}$ from equation (5), we also developed another linear model (meteorological model) through regression with wind speed u and v and other meteorological variables (water vapor W and surface pressure P_s). The goal here is to show that the regression based on the equation (5) or optical approach, which is based on the radiative transfer theory, can provide better estimate of surface $PM_{2.5}$ than the empirical approach using meteorological variables only.

Leave-one-out cross validation technique is applied to evaluate the predictive potential of linear regression models (Wilks, 2011). At each site, assuming we have N sets of known variables (of $PM_{2.5}$, $f(rh)$, μ, W, I, and P_s), the linear regression analysis can be conducted N times (assuming normality of the residuals), and each time, only N-1 sets of variables be used in the regression while leaving one set of variables out for evaluating the regression. By doing so, we have a total of 5N independent data points (and trials) to evaluate the robustness of equation (5). Note, because $f(rh)$ and μ are known variables and physically the left side of the equation (5) represents the optical path of aerosol, we use left size of equation as the dependent variable in regression for each site. This cross-evaluation is a first step to evaluate the potential of using DNB to estimate surface $PM_{2.5}$.

3. Results

3.1. Case demonstration

We first show two sets of paired images, one set focusing on nights with moonlight, and another set focusing on moonless nights. In each set, one nadir image with high $PM_{2.5}$ (larger than 10 $\mu g\ m^{-3}$) and small moonphase angle (stronger moonlight, Fig. 2c or 2d) is paired and contrasted with another edge-view image with low $PM_{2.5}$ (less than 8 μgm^{-3}) and large moonphase angle (weaker moonlight, Fig. 2a or 2b). For each set, if the atmospheric conditions of aerosols are the same, the nadir view image (Fig. 2c, d), because of their shorter radiative path length (e.g., airmass factor), would be brighter than their counterparts of edge view images (Fig. 2a, b). However, the opposite is true, as shown in Fig. 1, which indicates that the DNB is sensitive to the change of $PM_{2.5}$ at the surface. The smaller intensity of light in nadir view images on 25 October (Fig. 2c) and 17 August 2012 (Fig. 2d) can only be attributed to higher surface $PM_{2.5}$ concentration in these two days (as compared respectively to images Fig. 2a and b for 24 Sep. and 15 Sep. 2012). Quantitatively, large reduction of visible lights can be seen in urban centers and suburb regions where light sources at the surface are strong (Fig. 2e, f), while only a marginal difference can be found in rural areas that do not have city lights (Fig. 2e). This quantitative contrast suggests that city lights amplify the signal of aerosols in radiative extinction, enabling the change of $PM_{2.5}$ to be detectable from DNB.

3.2. Daily representativeness of $PM_{2.5}$ during VIIRS night overpass time

In 3-month averages for each hour, site E shows minimal diurnal variation, when compared to sites A-D (Fig. 2). Site E is the location for the GADNR NCore site, and is located southeast of the urban core. The NCore site was designed to assess transport from the urban core and secondary pollutant formation (GADNR, 2014), a reason for the more constant hourly profile versus sites A-D. Sites

A-D exhibit the consistent diurnal variation of surface $PM_{2.5}$ (Fig. 3): (a) sharp increase from 4:00 to 8:00 a.m. reflecting effects due to local traffic, the shallow boundary layer, and buildup of aerosol precursors at night; (b) progressive decrease between 8:00 a.m. to 2:00 p.m. reflecting the growth of the day-time boundary layer and influence of strong turbulent mixing; (c) slow increase between 2:00–8:00 pm reflecting again the increase of traffic and weakening of boundary layer mixing toward evening; (d) nearly constant (with slightly decrease) in 8:00 pm–4:00 am reflecting the stable nocturnal boundary layer. Such a diurnal variation pattern is indeed typical over the urban areas in the southeastern part of United States (Wang and Christopher, 2003). As a result of this diurnal variation pattern, $PM_{2.5}$ mass during VIIRS overpass time at night (~1:00 am local time) is representative of the 24-h mean of $PM_{2.5}$ within the deviation of less than 10% on average in 3 months (Fig. 3), which favors the use of VIIRS DNB to derive surface $PM_{2.5}$ for regional and daily-to-seasonal air quality evaluations. In addition, as expected, the suburb $PM_{2.5}$ concentrations (sites A, B, and C) are on average 2–4 μgm^{-3} smaller than those of urban centers (D and E). It is noted in Fig. 3 that $PM_{2.5}$ in mid-morning (10:00 am) is also representative of daily mean of PM2.5, and this time corresponds well with the MODIS/Terra satellite overpass time (Wang and Christopher, 2003). Further analysis (Fig. 4) shows that $PM_{2.5}$ at 1:00 locale time is highly correlated with corresponding daily mean $PM_{2.5}$ ($R = 0.82$) with mean bias of -0.1 $\mu g\ m^{-3}$ and root-mean-square error (RMSE) of 3.1 $\mu g\ m^{-3}$; in contrast, R, mean bias, and RMSE between $PM_{2.5}$ at 13:00 (e.g., VIIRS and MODIS/Aqua daytime overpass) and the daily mean are 0.75, -1.9 $\mu g\ m^{-3}$, and 3.5 $\mu g\ m^{-3}$, respectively. This contrast suggests that $PM_{2.5}$ derived from VIIRS DNB at night, if accurate, is more representative than the counterparts from VIIRS and MODIS/Aqua daytime data for assessing daily-mean air quality.

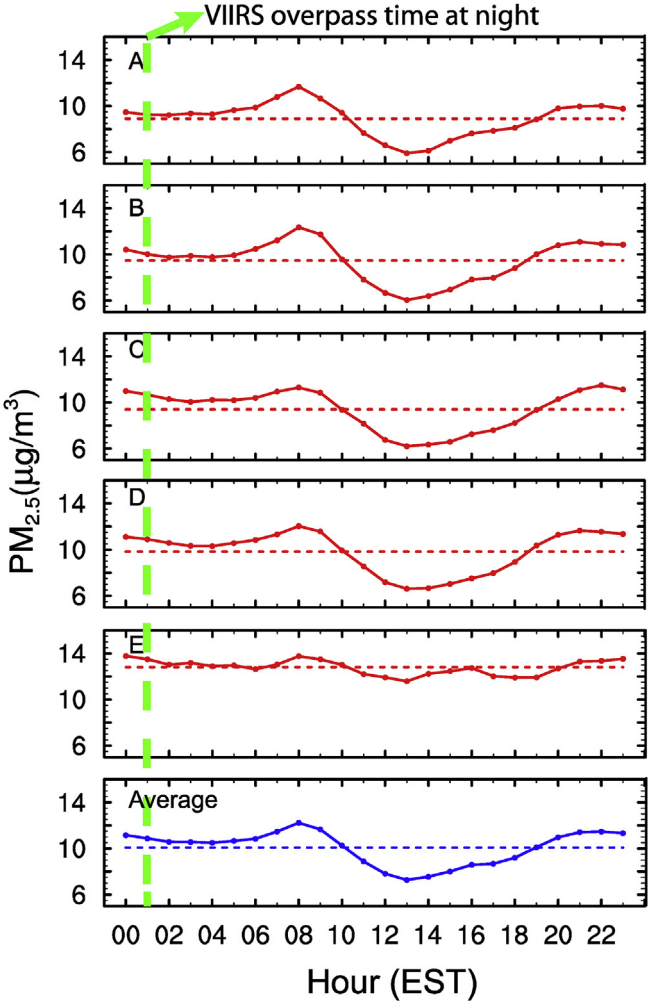

Fig. 3. Diurnal variation (solid line) and daily mean (dot line) of 3-month (August–October 2012) averages of hourly $PM_{2.5}$ mass concentration at 5 EPA monitoring sites in Atlanta. The location for site A-E is shown in Fig. 1. The bottom panel is similar as panel A but for the mean of data collected at all stations. Also overlaid (in green line) is the normal VIIRS overpass time at night. (For interpretation of the references to color in this figure legend, the reader is referred to the web version of this article.)

3.3. Regression analysis

Following equation (5), we first analyze the variables that should be included in the regression prediction of surface $PM_{2.5}$. Table 2 shows that while different variables have different correlations with the left-side term of eq. (5) at each site, *lnI* is the *only* variable that has either the largest or second largest statistically significant (negative) correlation with the left-side term of equation (5) over all sites, which suggests that *lnI* should be an indispensable part in our multiple regression for modeling $PM_{2.5}$. In contrast, the change of surface pressure was the only variable that shows neither the largest nor second largest correlation with the optical term for $PM_{2.5}$. Other variables such as water vapor (W), u, and v can also be useful for predicting $PM_{2.5}$, but their importance varies by site (as in Table 2). Note, to have the correlation analysis results in one table (Table 2), we show the correlation coefficients of $u \times f(rh)/\mu$ and $v \times f(rh)/\mu$ with $PM_{2.5} \times f(rh)/\mu$ (e.g., left-side of equation 5 assuming $Q_{ext}H$ as constant); similar results are found when correlation coefficients are computed for u (or v) and $PM_{2.5}$. The positive correlation between precipitiable water and surface $PM_{2.5}$ is consistent with some early studies that showed surface $PM_{2.5}$ is positively correlated with AOD that in turn is positively correlated with precipitiable water (Wang and Christopher, 2003; Smirnov et al., 2000). Interestingly, while horizontal wind (u) is negatively correlated surface $PM_{2.5}$ (Table 2), meridional wind (v) shows positive correlation, likely reflecting more polluted source from the south.

It should be noted that equation (5) or optical model is based on the physics that governs the radiative transfer, although many assumptions are made in the derivation of equation (5). Hence, the first step for construction of multiple-variable regression for the optical model is to include those most significant variables (such as *lnI*) in the model (or equation (5)). We didn't include u and v in the optical model because they are not part of the physics affecting the radiative transfer. Instead, they together with water vapor and surface pressure are included in another regression model that estimates the surface $PM_{2.5}$ purely based upon the meteorological variables.

Following the leave-out-one cross validation strategy, Fig. 5a presents the inter-comparison between $PM_{2.5}$ estimates from the multiple regression based on the optical model (as described in equation (5)) and the counterparts from the ground measurements. Overall, the predicted $PM_{2.5}$ (y) and observed (x) show a linear correlation coefficient R of 0.67 and a best-fit equation of $y = 0.996\ x + 0.044$. The overall bias in the prediction is close to zero (mean ± standard deviation of x: 10.89 ± 5.54 and y: 10.96 ± 5.52). These statistics are all better than the counterparts (Fig. 5b) from the multiple regression model using meteorological variables only (e.g., R of 0.5 and a best-fit equation of $y = 0.921\ x + 0.477$, and mean bias of -0.39). This result highlights the potential of applying the city-light data from satellite into the geospatial modeling of $PM_{2.5}$ at night.

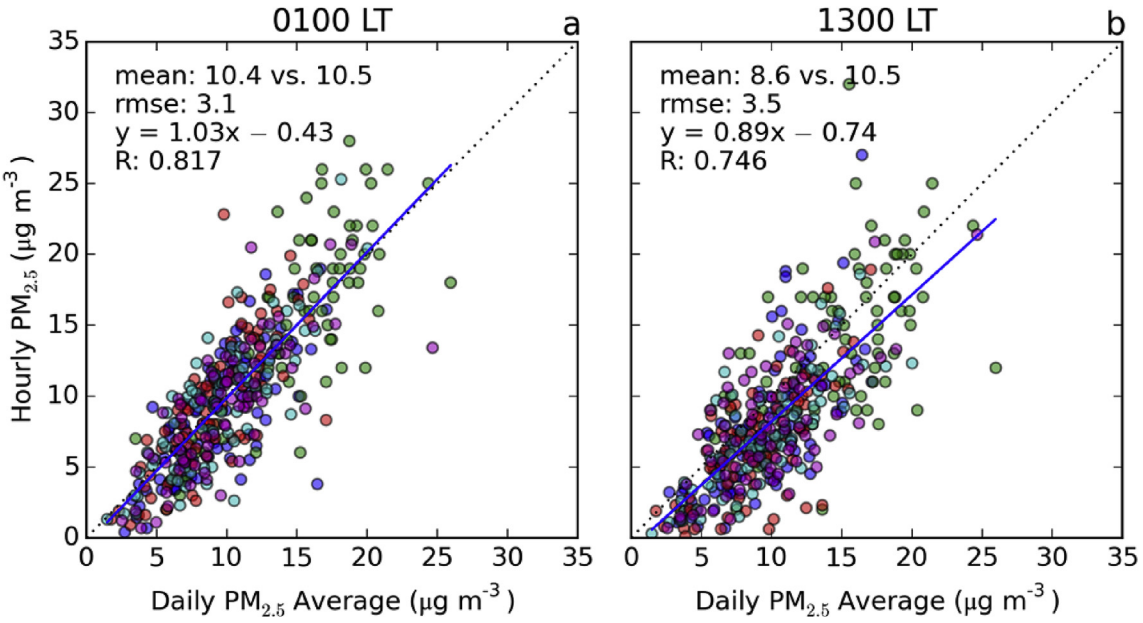

Fig. 4. (a) Inter-comparison between daily-mean (x-axis) $PM_{2.5}$ concentration and the corresponding $PM_{2.5}$ concentration measured at local time (LT) 1:00 (y-axis). (b) same as (a) except for $PM_{2.5}$ concentration measured at LT 13:00 (y-axis). The comparison is based on ground-based observations at sites A-E during during August–October 2012 in Atlanta, GA. Each circle represents data measured at one ground site on a particular day and is filled with same color for the same site. See text for details.

Table 2
Correlation coefficients (R) between $PM_{2.5} \times f(rh)/\mu$ and different variables at 6 ground sites (A-F as described in Table 1 and marked in Fig. 2)[a].

	A	B	C	D	E	F(CTR)
Variables\R						
lnI	**−0.78**	**−0.56**	***−0.53***	***−0.39***	**−0.71**	**−0.73**
ΔPs	0.05	0.21	0.08	0.14	0.10	0.10
W	0.49	0.38	**0.85**	0.17	0.00	0.10
$u \times f(rh)/\mu$	−0.21	−0.08	−0.21	−0.30	***−0.60***	***−0.66***
$v \times f(rh)/\mu$	***0.59***	***0.49***	0.48	**0.53**	0.54	0.52

[a] At each site, the largest value is in bold and second largest value is in the italic bold.

4. Summary and discussions

We presented a pilot study to illustrate the potential of using VIIRS DNB for particulate matter air quality monitoring at night. The case study focused on the moonless and cloudless nights in Atlanta during August–October 2012. We showed that, among 5 variables (including u and v component of wind speed, surface pressure, and columnar water vapor amount), the change of light intensity from VIIRS DNB is always among the top two variables that have the highest correlation with the change of measured surface $PM_{2.5}$. This is also consistent with results from our

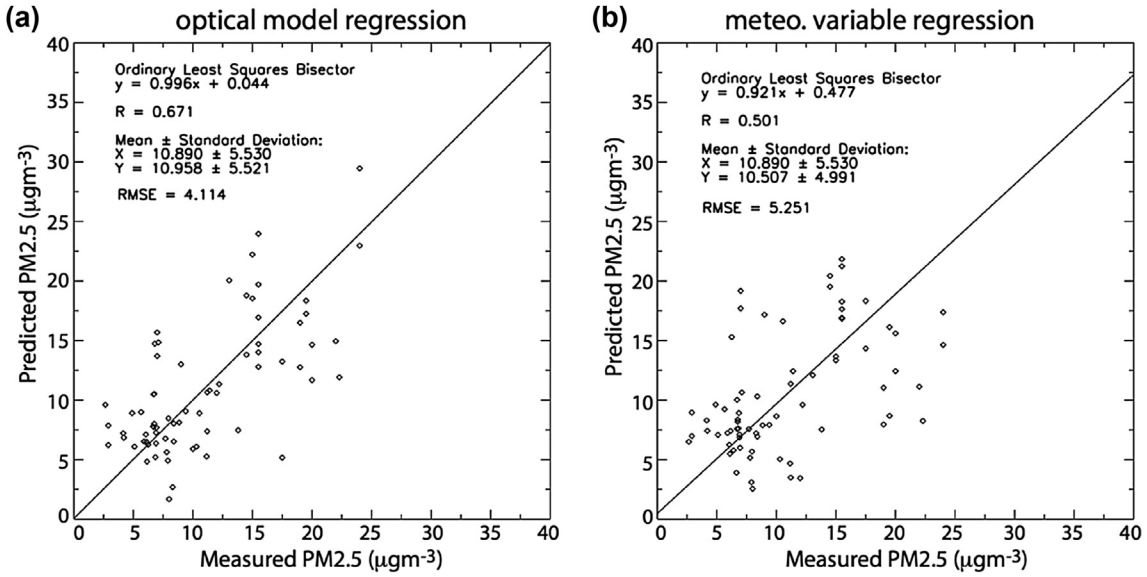

Fig. 5. Inter-comparison between predicted (y-axis) and measured (x-axis) $PM_{2.5}$. The prediction is based upon two models: (a) the optical model that includes variables of DNB radiance, surface pressure, and columnar water vapor (as described in equation (5)); and (b) the linear regression model based on surface meteorological variables (u and v wind, water vapor, and surface pressure) only. Each of those measured $PM_{2.5}$ data points in x-axis is excluded in the regression that predicts the corresponding $PM_{2.5}$ in y-axis (e.g., leave-one-out cross validation).

radiative transfer modeling that suggests the high sensitivity of DNB to the change of aerosols (and much less sensitivity of DNB to the change of water vapor) in the atmosphere illuminated by commonly-used outdoor lamps (such as high pressure sodium, LED and fluoresces lights). Under the assumption that Beer's Law is valid for analyzing the transfer of surface light through the atmosphere to space and the variation of the relationship between AOD and surface $PM_{2.5}$ is minimal at night (although varies spatially), a simple linear regression model is constructed to relate the DNB-measured light intensity to the GADNR-measured surface $PM_{2.5}$. The coefficients needed in this regression model can be obtained by using spatially and temporally paired surface $PM_{2.5}$ data, meteorological variables, and DNB data. Cross validation shows that the regression model can estimate the surface $PM_{2.5}$ with nearly no bias and a linear correlation coefficient of 0.67. While the potential of using DNB data to estimate surface $PM_{2.5}$ is demonstrated, several challenges should be addressed in future studies toward automatically mapping surface $PM_{2.5}$ at night from space. We outline these challenges and provide some strategies for thought in below.

First, a radiative transfer model that can account for the atmospheric transfer of both moonlight and surface-leaving visible light simultaneously is highly needed. Construction of such a model appears technically feasible, because (a) the code and database for a moonlight source function has been compiled by Miller and Turner (2009) and (b) several radiative transfer models, under the framework of discrete coordinate for a multi-layered plane-parallel medium, have been developed recently to account for surface-leaving radiances (especially those water-leaving radiances for ocean color retrievals, Spurr, 2006; Wang et al., 2014).

Second, spatial and temporal characterization of city light sources needs to be improved. The source function of city light is a function of bulb types as well as the light interaction with the surface that in turn depends on the altitude of these bulbs and the layout of their surrounding buildings and canopies. However, similar as the way that surface canopy and buildings are treated as one layer of the planar boundary (characterized by bi-directional reflectance function or BRDF) in the current radiative transfer model for satellite remote sensing, we think it is necessary to characterize the nighttime visible radiances coming out from the surface layer at different angles. A dedicated field campaign with multi-angle instrument capability can be a good start to pursue this.

Finally, many challenges in the use of daytime satellite data to estimate surface $PM_{2.5}$ still remain (in the nighttime), including the lack of a measurement-based aerosol extinction profile that links AOD to surface $PM_{2.5}$, conversion of ambient aerosol mass to dry aerosol mass that requires an account of aerosol hygroscopic growth and thereby knowledge of aerosol composition, as well as estimated dry surface $PM_{2.5}$ from total aerosol mass (Wang et al., 2010). Existing measurements for these compounding factors often lack spatial or temporal coverage, and therefore, it is foreseeable that a combination of satellite and chemistry transport models is highly needed for operational estimates of surface $PM_{2.5}$ from satellite data.

Disclaimer

The research described in this article has been reviewed by the National Exposure Research Laboratory, U.S. Environmental Protection Agency and approved for publication. Approval does not signify that the contents necessarily reflect the views and the policies of the Agency nor does mention of trade names or commercial products constitute endorsement or recommendation for use.

Acknowledgment

This study is supported by the NASA Applied Science Program (NNX11AJ03G) managed by John A. Haynes and the Suomi-NPP program managed by Diane Wickland and Paula Bontempi. We acknowledge Mr. Zhifeng Yang for his assistance in data analysis.

References

Al-Saadi, J., Szykman, J., Pierce, R.B., Kittaka, C., Neil, D., Chu, D.A., Remer, L., Gumley, L., Prins, E., Weinstock, L., MacDonald, C., Wayland, R., Dimmick, F., Fishman, J., 2005. Improving national air quality forecasts with satellite aerosol observations. Bull. Am. Met. Soc. 86, 1249–1261.

Cao, C., Xiong, J., Blonski, S., Liu, Q., Uprety, S., Shao, X., Bai, Y., Weng, F., 2013. Suomi NPP VIIRS sensor data record verification, validation, and long-term performance monitoring. J. Geophys. Res. Atmos. 118 (20), 11,664–11,678.

Dubovik, O., Holben, B., Eck, T.F., Smirnov, A., Kaufman, Y.J., King, M.D., Tanre, D., Slutsker, I., 2002. Variability of absorption and optical properties of key aerosol types observed in worldwide locations. J. Atmos. Sci. 59 (3), 590–608.

Elvidge, C.D., Baugh, K.E., Dietz, J.B., Bland, T., Sutton, P.C., Kroehl, H.W., 1999. Radiance calibration of DMSP-OLS low-light imaging data of human settlements. Remote Sens. Environ. 68 (1), 77–88.

Elvidge, C.D., Keith, D.M., Tuttle, B.T., Baugh, K.E., 2010. Spectral identification of lighting type and character. Sensors 10 (4), 3961–3988.

Engel-Cox, J., Kim Oanh, N.T., van Donkelaar, A., Martin, R.V., Zell, E., 2013. Toward the next generation of air quality monitoring: particulate matter. Atmos. Environ. 80, 584–590.

Georgia Department of Natural Resources, 2014. Enviromental Protection Division, Ambinet Air Monitoring Plan. www.air.dnr.state.ga.us/amp/2014_Ambient_Air_Monitoring_Plan.pdf.

Gupta, P., Christopher, S.A., Wang, J., Gehrig, R., Lee, Y.-C., Kumar, N., 2006. Satellite remote sensing of particulate matter and air quality assessment over global cities. Atmos. Environ. 40, 5880–5892.

Hoff, R., Christopher, S.A., 2009. Remote sensing of particulate matter air pollution from space : have we reached the promised land? J. Air Waste Manage. Assoc. 59, 642–675.

Jackson, J.M., Liu, H., Laszlo, I., Kondragunta, S., Remer, L.A., Huang, J., Huang, H.-C., 2013. Suomi-NPP VIIRS aerosol algorithms and data products. J. Geophys. Res. Atmos. 118, 12,673–12,689. http://dx.doi.org/10.1002/2013JD020449.

Johnson, R.S., Zhang, J., Hyer, E.J., Miller, S.D., Reid, J.S., 2013. Preliminary investigations toward nighttime aerosol optical depth retrievals from the VIIRS Day/Night Band. Atmos. Meas. Tech. 6 (5), 1245–1255.

Kessner, A., Wang, J., Levy, R., Colarco, P., 2013. Remote sensing of surface visibility from space: a look at the United States East Coast. Atmos. Environ. 81, 136–147.

King, M.D., Menzel, W.P., Kaufman, Y.J., Tanre, D., Gao, B.-C., Platnick, S., Ackerman, S.A., Remer, L.A., Pincus, R., Hubanks, P.A., 2003. Cloud and aerosol properties, precipitable water and profiles of temperature and water vapor from MODIS. IEEE Trans. Geosci. Remote Sens. 41 (2), 442–458.

Kopp, T.J., Thomas, W., Heidinger, A.K., Botambekov, D., Frey, R.A., Hutchison, K.D., Iisager, B.D., Brueske, K., Reed, B., 2014. The VIIRS cloud mask: progress in the first Year of S-NPP owards a common cloud detection scheme. J. Geophys. Res. Atmos. 119, 2441–2456.

Lee, T.F., Miller, S.D., 2006. NASA MODIS previews NPOESS VIIRS capabilities. Weather Forecast. 21, 649–655.

Lee, T.E., Miller, S.D., Turk, F.J., Schueler, C., Julian, R., Deyo, S., Dills, P., Wang, S., 2006. The NPOESS VIIRS Day/Night visible sensor,. Bull. Am. Meteorological Soc. 87 (2), 191–199.

Liou, K.N., 2002. An Introduction to Atmospheric Radiation, second ed. pp, Orlando, FL, USA.

Liu, Y., Park, R.J., Jacob, D.J., Li, Q., Kilaru, V., Sarmat, J.A., 2004. Mapping annual mean ground-level PM 2.5 concentrations using multiangle imaging spectroradiometer aerosol optical thickness over the contiguous United States. J. Geophys. Res. 109, D23S10. http://dx.doi.org/10.1029/2004JD005025.

Malm, W.C., Sisler, J.F., Huffman, D., Eldred, R.A., Cahill, T.A., 1994. Spatial and seasonal trends in particle concentration and optical extinction in the United States. J. Geophys. Res. 99, 1357–1370.

Miller, S.D., Turner, R.E., 2009. A Dynamic Lunar spectral irradiance data set for NPOESS/VIIRS Day/Night band nighttime environmental applications. Geoscience Remote Sens. IEEE Trans. 47 (7), 2316–2329.

Miller, S.D., Mills, S.P., Elvidge, C.D., Lindsey, D.T., Lee, T.F., Hawkins, J.D., 2012. Suomi satellite brings to light a unique frontier of nighttime environmental sensing capabilities. Proc. Natl. Acad. Sci. U.S.A. 109 (39), 15706–15711.

Polivka, T., Hyer, E., Wang, J., Peterson, D., 2015. First global analysis of saturation artifacts in the VIIRS infrared channels and the effects of sample aggregation. IEEE Geoscience Remote Sens. Lett. 1262–1266.

Rea, M., Bullough, J., Akashi, Y., 2009. Several views of metal halide and high-pressure sodium lighting for outdoor applications. Light. Res. Technol. 41 (4), 297–320.

Smirnov, A., Holben, B.N., Dubovik, O., O'Neill, N.T., Remer, L.A., Eck, T.F., Slutsker, I., Savoie, D., 2000. Measurement of atmospheric optical parameters on U.S. Atlantic coast sites, ships, and Bermuda during TARFOX. J. Geophys. Res. 105, 9887–9901. http://dx.doi.org/10.1029/1999JD901067.

Seinfeld, J.H., Pandis, S.N., 2006. Atmospheric Chemistry and Physics : From Air Pollution to Climate Change, second ed. New York John Wiley and Sons, Inc., US. 1203.
Spurr, R., 2006. VLIDORT: a linearized pseudo-spherical vector discrete ordinate radiative transfer code for forward model and retrieval studies in multilayer multiple scattering media. J. Quantitative Spectrosc. Radiat. Transf. 102 (2), 316–342.
Schwab, J.J., Felton, H.D., Rattigan, O.V., Demerjian, K.L., 2006. New York state urban and rural measurements of continuous PM2.5 mass by FDMS, TEOM, and BAM. J. Air Waste Manage. Assoc. 56, 372–383.
van Donkelaar, A., Martin, R.V., Spurr, R.J.D., Drury, E., Remer, L.A., Levy, R.C., Wang, J., 2013. Optimal estimation for global ground-level fine particulate matter concentrations. J. Geophys. Res. Atmos. 118 (11), 5621–5636.
Wang, J., Christopher, S.A., 2003. Intercomparison between satellite-derived aerosol optical thickness and PM2.5 mass: implications for air quality studies. Geophys. Res. Lett. 30 (21), 2095. http://dx.doi.org/10.1029/2003GL018174.
Wang, J., Martin, S.T., 2007. Satellite characterization of urban aerosols: importance of including hygroscopicity and mixing state in the retrieval algorithms. J. Geophys. Res. 112, D17203,. http://dx.doi.org/10.1029/2006JD008078.
Wang, J., Xu, X., Spurr, R., Wang, Y., Drury, E., 2010. Improved algorithm for MODIS satellite retrievals of aerosol optical thickness over land in dusty atmosphere: implications for air quality monitoring in China. Remote Sens. Environ. 114, 2575–2583.
Wang, J., Xu, X., Ding, S., Zeng, J., Spurr, R., Liu, X., Chance, K., Mishchenko, M., 2014. A numerical testbed for remote sensing of aerosols, and its demonstration for evaluating retrieval synergy from a geostationary satellite constellation of GEO-CAPE and GOES-R,. J. Quantitative Spectrosc. Radiat. Transf. 146 (0), 510–528.
Wilks, D.S., 2011. Statistical Methods in the Atmospheric Sciences, 3 ed. Academic Press. 704 pp.
Wilson, R., Spengler, J., 1996. In: Particles in our Air: Concentrations and Health Effects. Harvard Univ. Press, p. 254.
Winker, D., Pelon, J., McCormick, M.P., 2002. The CALIPSO Mission: Aerosol and Cloud Observations from Space, Int. Coord., Gr. on Laser Atmos. Stud. (Québec, CA).
Zhang, J., Reid, J.S., Miller, S.D., Turk, F.J., 2008. Strategy for studying nocturnal aerosol optical depth using artificial lights. Int. J. Remote Sens. 29 (16), 4599–4613.